# NJC

## Accepted Manuscript

This is an *Accepted Manuscript*, which has been through the RSC Publishing peer review process and has been accepted for publication.

*Accepted Manuscripts* are published online shortly after acceptance, which is prior to technical editing, formatting and proof reading. This free service from RSC Publishing allows authors to make their results available to the community, in citable form, before publication of the edited article. This *Accepted Manuscript* will be replaced by the edited and formatted *Advance Article* as soon as this is available.

To cite this manuscript please use its permanent Digital Object Identifier (DOI®), which is identical for all formats of publication.

More information about *Accepted Manuscripts* can be found in the **Information for Authors**.

Please note that technical editing may introduce minor changes to the text and/or graphics contained in the manuscript submitted by the author(s) which may alter content, and that the standard **Terms & Conditions** and the **ethical guidelines** that apply to the journal are still applicable. In no event shall the RSC be held responsible for any errors or omissions in these *Accepted Manuscript* manuscripts or any consequences arising from the use of any information contained in them.

# Effective Exchange Coupling in Alternating-Chains

# of a $\pi$-Extended 1,2,4-Benzotriazin-4-yl[†‡]

Christos P. Constantinides,[a] Andrey A. Berezin,[a] Maria Manoli,[a] Gregory M. Leitus,[b] Michael

Bendikov,[b] Jeremy M. Rawson[c] and Panayiotis A. Koutentis[a,*]

[a]*Department of Chemistry, University of Cyprus, P.O. Box 20537, 1678 Nicosia, Cyprus. E-mail:*

*koutenti@ucy.ac.cy; Fax: +357 22892809; Tel: +357 22892783*

[b]*Department of Organic Chemistry, Weizmann Institute of Science, 76100 Rehovot, Israel*

[c]*Department of Chemistry & Biochemistry, University of Windsor, 401 Sunset Avenue, Windsor,*

*ON, Canada N9B 3P4*

[†] This manuscript is dedicated to the memory of Prof. Michael Bendikov.

[‡] Electronic supplementary information (ESI) available: Cyclic voltammetry, solid-state and solution EPR, crystal structure geometry, table of energies for the triplet and broken symmetry singlet states along with spin contaminations, crystallographic experimental details and crystallographic information file (CIF) for radical **1** (CCDC 953369). For ESI and crystallographic data in CIF or other electronic format see DOI:

**ABSTRACT**: Air stable 1,3,7-triphenyl-1,4-dihydrothiazolo[5′,4′:4,5]benzo[1,2-*e*][1,2,4]triazin-4-yl pack in 1D $\pi$ stacks made of radical pairs with alternate short and long interplanar distances. The magnetic susceptibility exhibits a broad maximum at $73 \pm 5$ K and is interpreted

in terms of an alternating antiferromagnetic Heisenberg linear chain model with an average exchange interaction of $J$ = -43.8 cm$^{-1}$ and an alternation parameter $\alpha$ = 0.3 ($g_{solid}$ = 2.0028). The enhanced overlap between the $\pi$-extended SOMO orbitals leads to strong antiferromagnetic interactions along the chains ($J_1$ = -87.6 cm$^{-1}$ and $J_2$ = -26.3 cm$^{-1}$).

## INTRODUCTION

The search of organic multifunctional materials has attracted considerable attention in recent years.[1] Persistent organic radicals have been intensively pursued as promising building blocks for such materials.[2] The presence of unpaired electrons in these molecules offers the potential to combine magnetic, charge transport and optical properties. Customizing and tuning these properties requires the development of "structure-property relationships" that help to understand the effects of molecular structure on solid-state packing and their resultant properties.

We recently engaged in a magneto-structural study of the 1,2,4-benzotriazinyl family of radicals which, despite their exceptional air and moisture stability, have received little attention.[3] As part of our studies we have explored the chemistry of 1,2,4-benzotriazine[4] and developed high yielding synthetic routes to a range of 1,2,4-benzotriazinyl derivatives functionalized at the C7 position of the benzo-fused ring.[5] A range of one-dimensional magnetic properties have been found,[6] however, in an effort to increase the dimensionality of the magnetic interactions we have also recently prepared imidazolo-, oxazolo- and thiazolo-fused benzotriazinyls.[5c,d] We anticipate that the extension of the $\pi$ acene core will provide an effective pathway for the exchange interactions. Herein we present the solid-state characterization of 1,3,7-triphenyl-1,4-dihydro-thiazolo[5′,4′:4,5]benzo[1,2-$e$][1,2,4]triazin-4-yl (**1**) and provide magnetostructural correlation

based on variable-temperature (VT) magnetic susceptibility data, the X-ray structure and DFT calculations.

## EXPERIMENTAL

### General

Synthesis of radical **1** was previous reported.[5c] Melting points were determined using a TA Instruments DSC Q1000 with samples hermetically sealed in aluminum pans under an argon atmosphere, using heating rates of 5 °C/min. Solvents used for recrystallization are indicated after the melting point. UV spectra were obtained using a Perkin-Elmer Lambda-25 UV/*vis* spectrophotometer and inflections are identified by the abbreviation "inf". IR spectra were recorded on a Shimidazu FTIR-NIR Prestige-21 spectrometer with Pike *Miracle* Ge ATR accessory and strong, medium and weak peaks are represented by s, m and w, respectively. Low resolution (EI) mass spectra were recorded on a Shimadzu Q2010 GCMS with direct inlet probe. MALDI-TOF MS were conducted on a Bruker BIFLEX III time-of-flight (TOF) mass spectrometer. Cyclic voltammetry (CV) measurements were performed on a Princeton Applied Research Potentiostat/Galvanostat 263A apparatus. The concentration of the benzotriazinyl radical used was 1 mM in DCM. A 0.1 M DCM solution of tetra-*n*-butylammonium tetrafluoroborate (TBABF$_4$) was used as electrolyte. The reference electrode was Ag/AgCl and the scan rate was 50 mV/s. Ferrocene was used as an internal reference; the $E_{1/2}$(ox) of ferrocene in this system was 0.352 V.[6] EPR spectra were recorded on a Bruker EMXplus X-band EPR spectrometer at room temperature on solid state sample of the benzotriazinyl **1** and on dilute solutions in DCM. For the dilute solution spectra, the microwave power was in the region 5 − 70 mW with modulation frequencies of 50 or 100 kHz and modulation amplitudes of 0.5 − 1.0 G$_{pp}$.

Simulations of the solution and solid-state spectra were made using Winsim.[7] Magnetic properties were studied using a Quantum Design SQUID MPMS$_2$ field-shielded magnetometer. The DC (direct current) magnetic moment was measured on a 62.2 mg sample of radical **1**, which was placed in a gelatin capsule held by polyethylene straw. The magnetic susceptibility was measured in the temperature region 5 − 300 K in an applied field of 0.4 T. Data were collected in both warming and cooling modes with no significant differences in sample susceptibility. Data were corrected using a diamagnetic contribution of $\chi_{dia}$ = -150 × 10$^{-3}$ emu mol$^{-1}$. X-ray data of radical **1** (CCDC 953369) were collected on an Oxford-Diffraction Supernova diffractometer, equipped with a CCD area detector utilizing Mo-K$\alpha$ radiation ($\lambda$ = 1.5418 Å). A suitable crystal was attached to glass fibers using paratone-N oil and transferred to a goniostat where they were cooled for data collection. Unit cell dimensions were determined and refined by using 2746 (4.06 ≤ θ ≤ 72.44º) reflections. Empirical absorption corrections (multi-scan based on symmetry-related measurements) were applied using CrysAlis RED software.[8] The structures were solved by direct method and refined on $F^2$ using full-matrix least squares using SHELXL97.[9] Software packages used: CrysAlis CCD[8] for data collection, CrysAlis RED[8] for cell refinement and data reduction, WINGX for geometric calculations,[10] and Mercury 3.1[11] for molecular graphics. The non-H atoms were treated anisotropically. The hydrogen atoms were placed in calculated, ideal positions and refined as riding on their respective carbon atoms. DFT single-point calculations were carried out on the X-ray crystallographically determined geometry to calculate the energies of the triplet ($E_T$) and broken symmetry singlet ($E_{BS}$) states. Calculations were performed using the Gaussian 03 suite of programs, Rev C.02 for the UB3LYP functional and Gaussian 09 suite of programs, Rev. D.01 for the UMO6-2X and UX3LYP functionals.[12,13]

**Spectral analysis for radical 1:**

1,3,7-Triphenyl-1,4-dihydrothiazolo[5',4':4,5]benzo[1,2-e][1,2,4]triazin-4-yl (**1**)[5c]

   Black needles (74 mg, 74%), mp (DSC) onset: 253.1 $^o$C, peak max: 260.3 $^o$C, decomp. onset: 298.2 $^o$C, peak max: 327.1 $^o$C (from PhH), $R_f$ 0.36 (Et$_2$O/$n$-hexane, 1:1); (found: C, 74.90; H, 4.01; N, 13.36. C$_{26}$H$_{17}$N$_4$S requires C, 74.80; H, 4.10; N, 13.42%); $\lambda_{max}$(DCM)/nm 259 inf (log $\varepsilon$ 3.52), 282 inf (3.67), 304 (3.72), 365 (2.86), 402 inf (3.34), 423 (3.48), 470 (2.70), 514 (2.65), 561 (2.66), 660 inf (2.42); $v_{max}$/cm$^{-1}$ 3067w, 3057w and 3019w (Ar CH), 1589w, 1530w, 1506w, 1491m, 1479m, 1458s, 1439s, 1391s, 1346m, 1317w, 1287w, 1258m, 1225m, 1204w, 1182w, 1169w, 1157w, 1136w, 1067w, 1045w, 1024m, 1001w, 982w, 955m, 926w, 912w, 854s, 826m, 797m, 787m, 779m, 770w, 756s; $m/z$ (EI) 417 (M$^+$, 100%), 401 (3), 341 (4), 314 (9), 209 (30), 180 (7), 177 (3), 167 (4), 165 (3), 139 (4), 106 (8), 77 (27), 69 (3), 62 (6), 51 (8).

**RESULTS AND DISCUSSION**

**Synthesis**

   Radical **1** was prepared in three steps beginning from the benzotriazin-7($H$)-one **2** in an overall yield of 50%:[5c] The benzotriazinone **2** is directly aminated using $O$-benzylhydroxylamine hydrochloride and Hünig's base in refluxing ethanol to give the 6-aminobenzotriazinone **4** in 79% on a multigram scale (Scheme 1). Subsequent reaction of the 6-aminobenzotriazinone **4** with benzoyl chloride and NaH (1.2 equiv.) in DMF at *ca*. 20 $^o$C for 12 h gave the $N$-(benzo-triazin-6-yl)carboxamide **5** in 86% yield. Treating the carboxamide **5** with P$_2$S$_5$ (1 equiv.) in refluxing PhMe gave the 1,3,7-triphenylthiazolobenzotriazinyl **1** in 74% (Scheme 1).
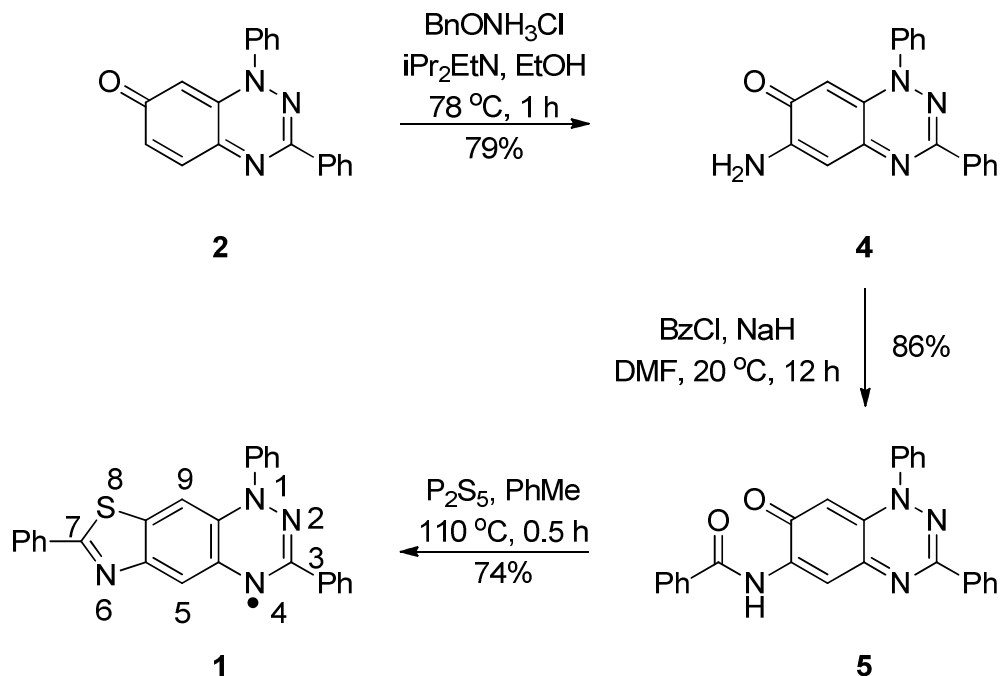
**Scheme 1.** Synthetic Route to the 1,3,7-triphenylthiazolobenzotriazinyl **1**

**EPR and Cyclic Voltammetry**

The redox behaviour of radical **1** is similar to that of other benzotriazinyl radicals,[3,14] exhibiting two fully reversible waves which correspond to the -1/0 and 0/+1 processes (Figure S1 in the ESI). The oxidation potential occurred at $E_{1/2}^{0/+1}$ = 0.21 V *vs* ferrocene/ferrocenium couple, whereas the reduction potential occurred at $E_{1/2}^{-1/0}$ = -0.87 V. Room temperature solid-state EPR spectra on radical **1** revealed essentially isotropic singlet EPR spectrum ($g_{solid}$ = 2.0028) consistent with an organic radical with little spin-orbit coupling (Figure S2 in the ESI). In solution the *g*-factor of the radical ($g_{soln}$ = 2.0024) was similar to the one observed in the solid-state but the lower concentration permitted the resolution of the ^{14}N hyperfine coupling to the three chemically distinct N atoms of the triazinyl ring (Figure S3 in the ESI). The similarity in $a_N$ values led to the spectrum typically appearing as a non-binomial 7-line multiplet, though full

simulation revealed subtle differences in the hyperfine coupling constants (hfcc). Previous EPR and ENDOR studies by Neugebauer on $^{15}$N-labelled benzotriazinyl radicals showed that $a_{N1} \gg a_{N4} > a_{N2}$.[3d,15] Assignment of hfcc for radical **1**, extracted from simulated first-derivative spectra, are given according to Neugebauer's reported trend; $a_{N1} = 6.48$, $a_{N2} = 4.80$ and $a_{N4} = 5.25$ G. Spin densities estimated based on hfcc using McConnell's equation are $\rho_{N1} = 0.259$, $\rho_{N2} = 0.226$ and $\rho_{N4} = 0.248$.[16,17]

**Crystal Structure**

Suitable single crystals of **1** for X-ray diffraction studies were obtained by slow diffusion of *n*-pentane into a benzene solution of the radical. Radical **1** crystallizes in the triclinic *P*-1 space group with one molecule in the asymmetric unit (see Figure S4 in the ESI for atom numbering used in the X-ray discussion). The intramolecular geometrical parameters are similar to previously studied benzotriazinyl radicals.[3,14] The phenyl substituents at C1 (3-Ph) and C8 (7-Ph) are close to planarity with dihedral angles of 0.4(4)$^{o}$ and 7.1(4)$^{o}$, respectively. The thiazole ring is also planar with interatomic distances and angles typical of other benzothiazoles; S1-C6, 1.736(2) Å; N4-C7, 1.387(3) Å and C8-S1-C6, 89.1(2)$^{o}$; C8-N4-C7, 110.8(2)$^{o}$.
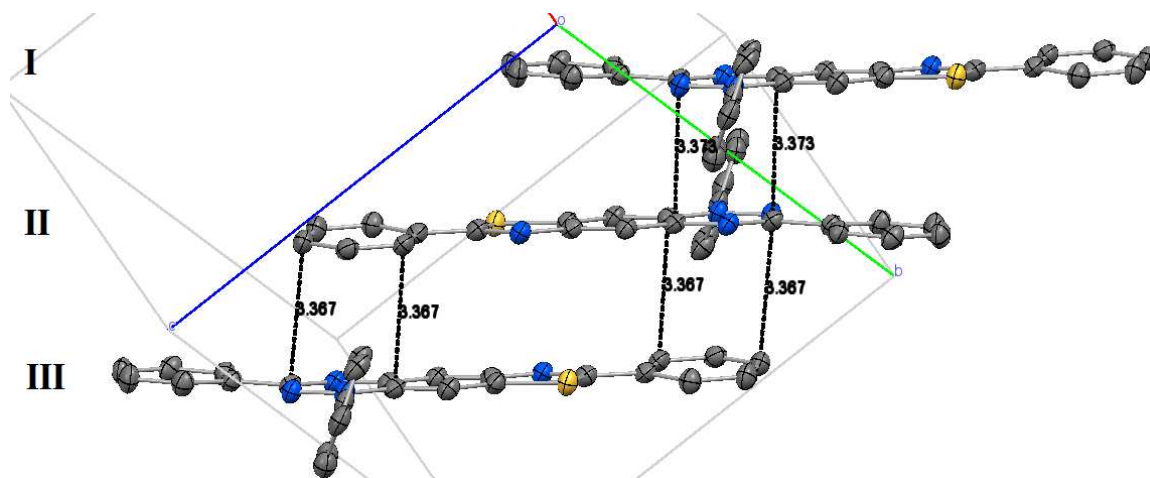
**Figure 1.** Packing diagram of radical **1** along the *c* axis (hydrogens are omitted for clarity). Thermal ellipsoid are at 50% probability. Shortest intermolecular contacts: pair I-II [$d_{C1\cdots C2}$ = 3.373(4) Å, (-x, 1-y, -z)] and pair II-III [$d_{C1\cdots C12}$ = $d_{C3\cdots C14}$ = 3.367(4) Å, (-x, 1-y, 1-z)].

It is anticipated that the $\pi$-extended acene core of radical **1** will favour $\pi$-stacking and the enhanced orbital overlap will lead to stronger exchange interactions. Molecules of the 1,3,7-triphenylthiazolobenzotriazinyl **1** form 1D $\pi$-slipped stacked columns, with the mean interplanar distance between radicals alternating down the stack. This gives rise to a centrosymmetric pair (radicals I-II in Fig. 1) where the spin-bearing triazinyl rings are related through a centre of inversion and overlap *via* a pair of short face-to-face interactions [$d_{C1\cdots C2}$ = 3.373(4) Å, (-x, 1-y, -z)]. The structure of pair I-II is further supported by a pair of two crystallographically equivalent, weak C-H⋯N contacts between the triazinyl N3 and an *ortho*-hydrogen atom of the *N*-phenyl ring [$d_{C26\cdots N3}$ = 3.860(3) Å, (-x, 1-y, -z), C-H⋯N angle = 143°]. The centrosymmetric pairs I-II pack parallel to the crystallographic *c* axis and relate to each other *via* a centre of inversion running in the middle of the stacked thiazole rings; this places the triazinyl ring above the 7-Ph

and links pairs I-II *via* a set of equidistant C···C interactions [radical pair II-III in Fig. 1; $d_{C1···C12}$ = $d_{C3···C14}$ = 3.367(4) Å, (-x, 1-y, 1-z)].

Neighbouring stacks, pack along the *a* axis *via* a net of C-H···N contacts between the thiazolo N4 and the *para*-hydrogen atom of the *N*-phenyl ring [$d_{C24···N4}$ = 3.337(3) Å, (-1+x, -1+y, z), C-H···N angle = 131°; Fig. 2]. A tight packing with no voids is completed with edge-to-face $\pi$-contacts among the *N*-phenyl and the 3-/7-phenyl substituents.
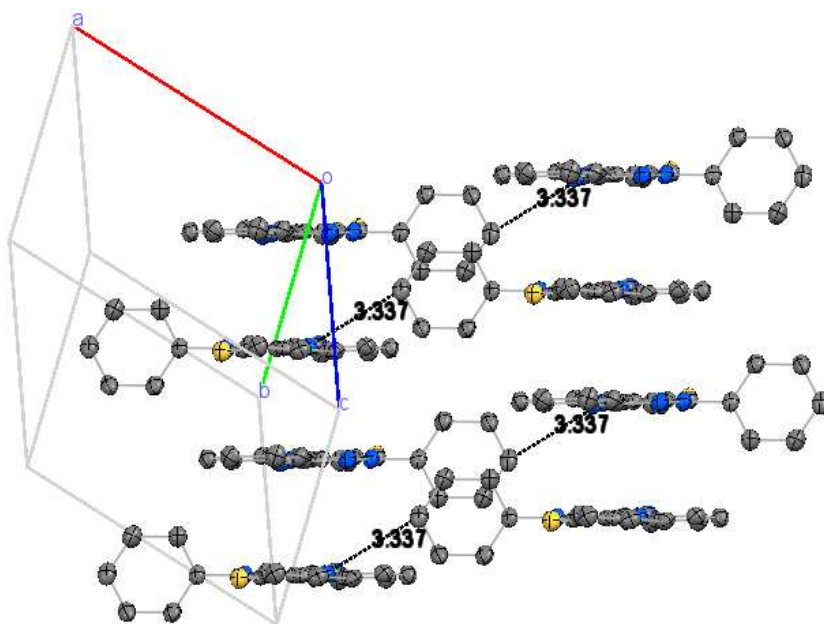


**Figure 2.** Packing of radical **1** along the *a* axis showing the interstack interactions (hydrogens are omitted for clarity and thermal ellipsoid are at 50% probability).

**Magnetic Properties**

The 1D $\pi$-slipped stacking of the 1,3,7-triphenylthiazolobenzotriazinyl **1** suggests uni-dimensional magnetic interactions that propagate parallel to the stacking direction, along which, the orbital overlap between the singly-occupied molecular orbitals is maximized. Variable-

temperature magnetic-susceptibility measurements on radical **1** were obtained by using a SQUID magnetometer in the temperature region 5 – 300 K in an applied field of 0.4 T. Data were collected in both warming and cooling modes with no significant differences in sample susceptibility. Data were corrected using a diamagnetic contribution of $\chi_{dia}$ = -150 × $10^{-3}$ emu $mol^{-1}$. The temperature dependence of $\chi$ and $\chi T$ for radical **1** is presented in Fig. 3. On cooling from 300 K, the molar susceptibility $\chi$ increases gradually and reaches a broad maximum at $T_{max}$ = 73 ± 5 K indicating strong antiferromagnetic interactions. After passing through the maximum, $\chi$ falls off gradually down to 20 K before it increases again at lower temperatures. The increase of $\chi$ below 20 K is attributed to uncoupled radicals at defect sites in the lattice. The alternating interplanar distances along the stacking direction ($d_{I-II}$ = 3.350 Å, $d_{II-III}$ = 3.393 Å) indicates that the appropriate model to fit the magnetic data is Hatfield's expression[18] for the magnetic susceptibility of Heisenberg alternating-chains of $S$ = ½ spins. The spin Hamiltonian for this model is:

$$H = -2J\sum_{i=1}^{n/2}\left[S_{2i}S_{2i-1} + \alpha S_{2i}S_{2i+1}\right]$$

Where $J$ and $\alpha J$ are the exchange integrals along the stacking direction and $\alpha$ is a parameter indicating the degree of alternation. At the extremes, when $\alpha = 0$ the model corresponds to an isolated dimer system and when $\alpha = 1$ the model reduces to the regular linear-chain model.
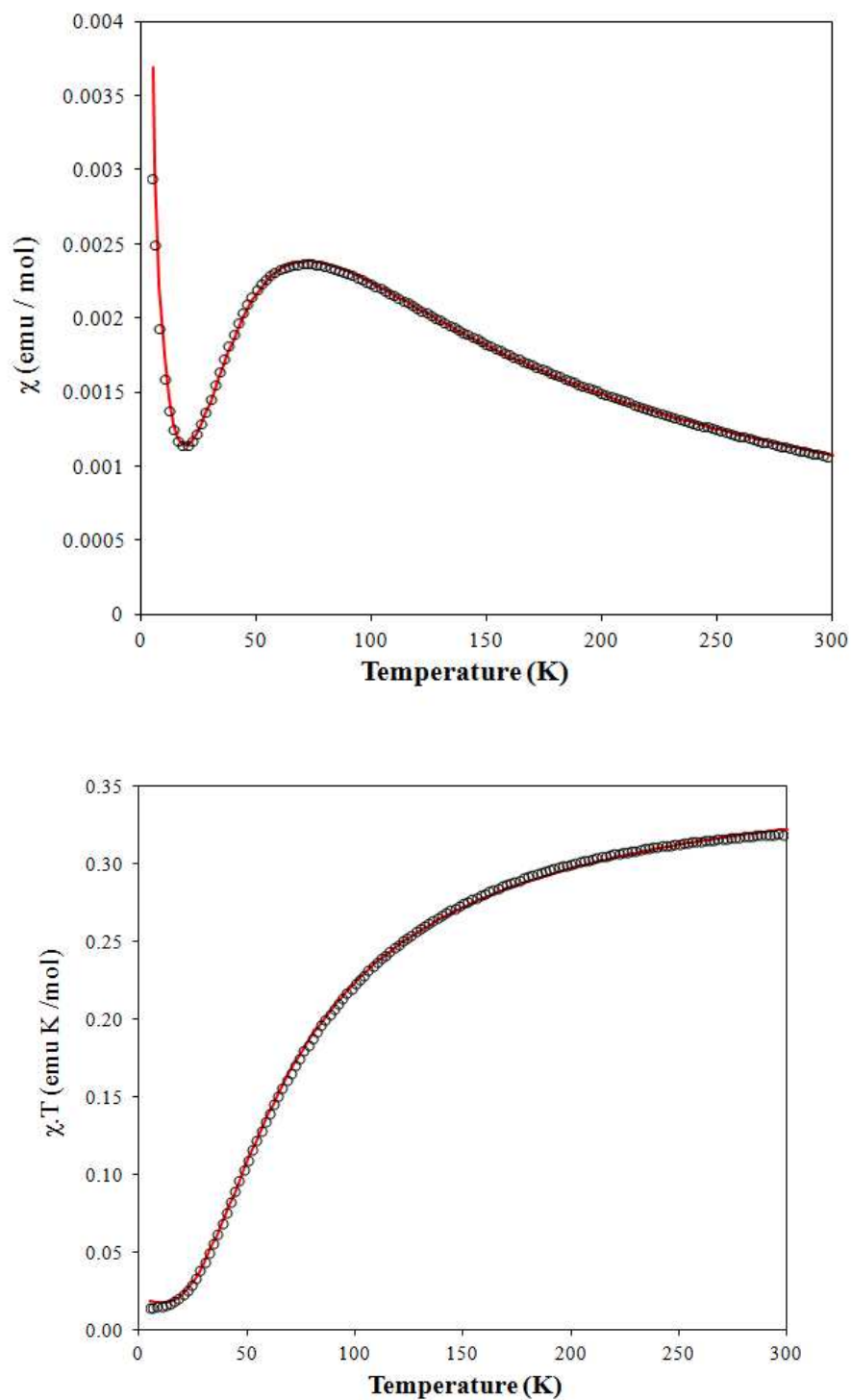
**Figure 3.** Temperature dependence of $\chi$ (top) and $\chi T$ (bottom) for radical **1**. The red line represents the best fit to the Heisenberg alternating linear-chain model[18] with $J = -43.8$ cm$^{-1}$, $\alpha = 0.3$, $\rho = 0.95$, $g_{solid} = 2.0028$.

11

The best fit to the magnetic susceptibility data was obtained using the set of polynomial parameters for $0 \leq \alpha \leq 0.4$. A parameter $\rho$ was included to account for the susceptibility arising from uncoupled radicals at the lattice defect sides. The fit reproduces well both the position and the maximum in $\chi$ when $J$ = -43.8 cm$^{-1}$, $\alpha$ = 0.3, $\rho$ = 0.95, $g_{solid}$ = 2.0028. By applying the ratio of $\alpha = J_2 / J_1$, where $J_1 = 2J$ and $J_2 = 2\alpha J$, we determined estimated $J_1$ and $J_2$ values along the chain direction of -87.6 and -26.3 cm$^{-1}$, respectively.

**Calculation of exchange interactions**

Exchange coupling within radical pair I-II is expected to be stronger since the radicals overlap predominantly over the spin-bearing triazinyl moieties maximizing the SOMO-SOMO interaction. Conversely the molecular arrangement in radical pair II-III brings the 7-phenyl ring, bearing little spin density (SOMO orbital coefficients are smaller, Fig. 4), on top of the adjacent triazinyl ring. Therefore, in the absence of other dominating exchange coupling interactions, $J_1$ and the weaker $J_2$ could be assigned to the interactions within radical pairs I-II and II-III, respectively.
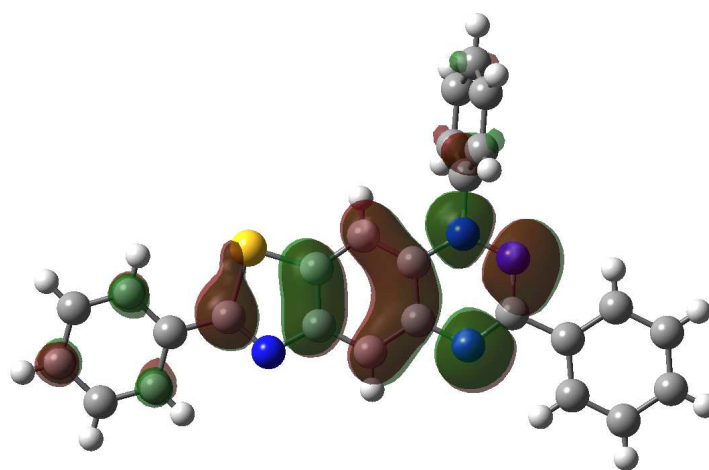


**Figure 4.** The calculated SOMO orbital of radical **1** at the UB3LYP/6-311G++(d,p) level of theory.

　　Direct estimates of the magnetic interactions within radical pairs can be obtained from quantum chemistry methods.[19] Although the macroscopic magnetic behaviour is the outcome of all existing magnetic interactions working together, for radicals with low dimensional magnetic topology, *e.g.*, 1,3,7-triphenylthiazolobenzotriazinyl **1**, computed exchange interactions can correlate in a qualitative way with experimentally determined exchange couplings.

　　The calculated spin-spin exchange interactions $J_{\text{I-II}}$ and $J_{\text{II-III}}$ were determined by the unprojected equation, $2J_{\text{DFT}} = 2(E_{\text{BS}} - E_{\text{T}})/2$.[20] The energies of the triplet ($E_{\text{T}}$) and broken symmetry singlet ($E_{\text{BS}}$) states were determined by single point calculations on crystallographically determined geometries of radical pairs I-II and II-III (Table T1 in the ESI).

**Table 1.** Calculated Exchange Interactions[a] of Pair I-II ($J_{\text{I-II}}$) and Pair II-II ($J_{\text{II-III}}$) on their X-Ray Determined Geometries at the UB3LYP Level of Theory.

| Basis Set | $J_{\text{I-II}}$ | $J_{\text{II-III}}$ | $J_1{}^{b}$ | $J_2{}^{b}$ |
|---|---|---|---|---|
| 6-311++G(d,p) | -46.6[c] | +6.6[c] | -87.6 | -26.3 |
| 6-311++G(2d,p) | -103.8[c] | -6.2[c] | | |
| 6-311++G(d,p) | -92.4[d] | +13.1[d] | | |
| 6-311++G(2d,p) | -205.6[d] | -12.4[d] | | |

[a] Exchange interactions are given in cm$^{-1}$.

[b] Experimentally determined exchange interactions in cm$^{-1}$.

[c] Calculated by the unprojected method.

[d] Calculated by the approximate projected method.

　　Although advanced and computationally expensive quantum chemical methods such as CASSCF and CASPT2 provide good results, DFT functionals such as the B3LYP perform well

in the computation of exchange interactions.[19] The latter method was employed for the calculations of $J_{I-II}$ and $J_{II-III}$ using the 6-311++G(d,p) and 6-311++G(2d,p) basis sets (Table 1).

Adding 2d functions on heavy atoms to take in account the presence of the S atom, at the UB3LYP/6-311++G(2d,p) level of theory using the unprojected method, successfully reproduced both the sign and magnitude of the magnetic exchange interactions ($J_{I-II}$ = -103.8 cm$^{-1}$ and $J_{II-III}$ = -6.2 cm$^{-1}$ *vs* $J_1$ = -87.6 cm$^{-1}$ and $J_2$ = -26.3 cm$^{-1}$). Calculations confirm the qualitative assignment of $J_1$ to pair I-II and $J_2$ to pair II-III, as $J_{I-II}$ > $J_{II-III}$ and $J_1$ > $J_2$. Although B3LYP combined with the unprojected method provides reasonable values for the exchange interactions within radical pairs, we screened two more hybrid meta-GGA functionals, X3LYP and MO6-2X, using the 6-311++G(2d,p) basis set. These two functionals provide better descriptions of non-bond interactions such as van der Waals, hydrogen bonding, $\pi$-$\pi$ stacking, charge-transfer complexes and dipole interaction complexes.[21] The values of the calculated exchange interactions at the UMO6-2X/6-311++G(2d,p) and UX3LYP/6-311++G(2d,p) level of theory were similar to the values obtained from the UB3LYP/6-311++G(d,p) method (Table 2). Applying the approximate projection method, $2J_{DFT} = 2(E_{BS} - E_T)/(<\hat{S}^2>_T - <\hat{S}^2>_{BS})$, which takes in account the overlap between the magnetic orbitals *via* the calculated eigenvalues of the $\hat{S}^2$ operator, the magnitude of the computationally and experimentally determined exchange interactions are in excellent agreement for the UB3LYP/6-311++G(d,p), UM06-2X/6-311++G(2d,p) and UX3LYP/6-311++G(2d,p) level of theories. Nevertheless, these functionals in combination with the approximate projected method, failed to reproduce the sign of the $J_{II-III}$.

**Table 2** Calculated Exchange Interactions[a] of Pair I-II ($J_{I-II}$) and Pair II-II ($J_{II-III}$) on their X-Ray Determined Geometries Using the UMO6-2X and UX3LYP Functionals.[b]

| Functional | $J_{I-II}$ | $J_{II-III}$ | $J_1{}^c$ | $J_2{}^c$ |
|---|---|---|---|---|
| UMO6-2X | $-47.4^d$ | $+11.2^d$ | -87.6 | -26.3 |
| UX3LYP | $-46.9^d$ | $+10.6^d$ | | |
| UMO6-2X | $-94.8^e$ | $+22.4^e$ | | |
| UX3LYP | $-92.9^e$ | $+21.1^e$ | | |

[a] Exchange interactions are given in $cm^{-1}$.

[b] Employing the 6-311++G(2d,p) basis set.

[c] Experimentally determined exchange interactions in $cm^{-1}$.

[d] Calculated by the unprojected method.

[e] Calculated by the approximate projected method.

**DISCUSSION**

The magnetic behaviour of 1,2,4-benzotriazinyls can be rationalized by using the molecular orbital (MO) model.[22] In the MO model the exchange coupling interaction ($J_{AB} = 2K_{ij} + 4c_{ij}S_{ij}{}^2$) is proportional to the size of the overlap between SOMO orbitals ($S_{ij}$). The sign of the exchange interactions depends primarily on the distance and orientation of the coupled radicals. In related $\pi$ systems, Oakley demonstrated that there is a fine balance between ferro- and antiferromagnetic interactions by adjusting the degree of slippage through chemical or mechanical pressure.[23] For 1,2,4-benzotriazinyls the latitudinal and longitudinal slippage angles as well as the distance between the radicals determine the nature of the interactions along the $\pi$-stacking direction.[14] A direct comparison with other 1,2,4-benzotriazinyls is not straight forward as these radicals pack in a variety of ways owing to a complex set of geometrical parameters that give rise to a range of

magnetic interactions. However, the magnitude of these magnetic exchange interactions is directly related to the degree of overlap between the SOMO orbitals, irrespective of their nature (either ferro- or antiferromagnetic). The magnitude of the exchange interactions of 1,3,7-triphenylthiazolobenzotriazinyl **1** ($J_1$ = -87.6 cm$^{-1}$ and $J_2$ = -26.3 cm$^{-1}$) is considerably larger than the exchange interactions of non-fused benzotriazinyls such as the 1D regular chains of the 1,3,7-triphenyl- and 1,3-diphenyl-7-(4-fluorophenyl)-1,4-dihydro-1,2,4-benzotriazin-4-yls with 2$J$ = -25.8 and -23.6 cm$^{-1}$.[14c] The $\pi$-extended acene core of thiazolo-fused radical **1** leads to an enhanced orbital overlap and therefore to stronger exchange interactions. While side-on intermolecular contacts connect neighbouring chains, they fail to increase the dimensionality of the magnetic interactions. The low dimensionality of the magnetic topology can be explained by the presence of phenyl groups around the periphery which isolate the spin-bearing units and prohibit interactions over the other two dimensions. If long-range ordering is to be realized then fine tuning of the substituents' steric effects is required to make the 1,2,4-benzotriazinyl core more available to the surrounding environment.

**CONCLUSIONS**

In conclusion, the crystal structure and magnetic properties of 1,3,7-triphenyl-1,4-dihydro-thiazolo[5′,4′:4,5]benzo[1,2-*e*][1,2,4]triazin-4-yl (**1**) have been investigated. The radicals $\pi$ stack in 1D columns along the *c* axis and comprise of radical pairs (I-II and II-III) with alternate short and long interplanar distances. Magnetic susceptibility measurements along with quantum chemical calculations reveal the existence of strong antiferromagnetic interactions within the 1D stacks, as a result of an enhanced overlap between the $\pi$-extended SOMO orbitals.

**REFERENCES**

1 I. Ratera and J. Veciana, *Chem. Soc. Rev.*, 2012, **41**, 303.

2 (*a*) D. A. Haynes, *CrystEngComm*, 2011, **13**, 4793; (*b*) O. A. Rakitin, *Russ. Chem. Rev.*, 2011, **80**, 647; (*c*) R. G. Hicks, *Org. Biomol. Chem.*, 2007, **5**, 1321; (*d*) S. Nakatsuji and H. Anzai, *J. Mater. Chem.*, 1997, **7**, 2161; (*e*) J. M. Rawson, A. Alberola and A. J. Whalley, *J. Mater. Chem.*, 2006, **16**, 2575.

3 (*a*) H. M. Blatter and H. Lukaszewski, *Tetrahedron Lett.*, 1968, **9**, 2701; (*b*) C. Krieger and F. A. Neugebauer, *Acta Crystallogr.*, 1996, **C52**, 3124; (*c*) A. T. Gubaidullin, B. I. Buzykin, I. A. Litvinov and N. G. Gazetdinova, *Russ. J. Gen. Chem.*, 2004, **74**, 939; (*d*) K. Mukai, K. Inoue, N. Achiwa, J. B. Jamali, C. Krieger and F. A. Neugebauer, *Chem. Phys. Lett.*, 1994, **224**, 569.

4 (*a*) T. A. Ioannou, P. A. Koutentis, H. Krassos, G. Loizou and D. Lo Re, *Org. Biomol. Chem.*, 2012, **10**, 1339; (*b*) P. A. Koutentis, H. Krassos and D. Lo Re, *Org. Biomol. Chem.*, 2011, **9**, 5228; (c) P. A. Koutentis, G. Loizou and D. Lo Re, *J. Org. Chem.*, 2011, *76*, 5793; (*d*) M. Demetriou, A. A. Berezin, P. A. Koutentis and T. Krasia-Christoforou, *Polym. Int.*, 2013, DOI: 10.1002/pi.4566.

5 (*a*) P. A. Koutentis and D. Lo Re, *Synthesis*, 2010, 2075; (*b*) C. P. Constantinides, P. A. Koutentis and G. Loizou, *Org. Biomol. Chem.*, 2011, **9**, 3122; (*c*) A. A. Berezin, C. P. Constantinides, C. Drouza, M. Manoli and P. A. Koutentis, *Org. Lett.*, 2012, **14**, 5586; (*d*) A. A. Berezin, C. P. Constantinides, S. I. Mirallai, M. Manoli, L. L. Cao, J. M. Rawson and P. A. Koutentis, *Org. Biomol. Chem.*, 2013, **11**, 6780.

6 M. Dietrich and J. Heinze, *J. Am. Chem. Soc.*, 1990, **112**, 5142.

7 Winsim 2002 (v.0.98), Public EPR Software Tools, D. A. O'Brien, D. R. Duling, Y. C. Fann, NIEHS, National Institutes of Health, USA.

8 Oxford Diffraction (2008). CrysAlis CCD and CrysAlis RED, version 1.171.32.15, Oxford Diffraction Ltd, Abingdon, Oxford, England.

9 G. M. Sheldrick, "SHELXL97-A program for the refinement of crystal structure", University of Göttingen, Germany.

10 L. J. Farrugia, *J. Appl. Cryst.*, 1999, **32**, 837.

11 C. F. Macrae, P. R. Edgington, P. McCabe, E. Pidcock, G. P. Shields, R. Taylor, M. Towler, and J. van de Streek, *J. Appl. Cryst.*, 2006, **39**, 453.

12 Gaussian 03, Revision C.02, M. J. Frisch, G. W. Trucks, H. B. Schlegel, G. E. Scuseria, M. A. Robb, J. R. Cheeseman, J. A. Montgomery, Jr., T. Vreven, K. N. Kudin, J. C. Burant, J. M. Millam, S. S. Iyengar, J. Tomasi, V. Barone, B. Mennucci, M. Cossi, G. Scalmani, N. Rega, G. A. Petersson, H. Nakatsuji, M. Hada, M. Ehara, K. Toyota, R. Fukuda, J. Hasegawa, M. Ishida, T. Nakajima, Y. Honda, O. Kitao, H. Nakai, M. Klene, X. Li, J. E. Knox, H. P. Hratchian, J. B. Cross, V. Bakken, C. Adamo, J. Jaramillo, R. Gomperts, R. E. Stratmann, O. Yazyev, A. J.

Austin, R. Cammi, C. Pomelli, J. W. Ochterski, P. Y. Ayala, K. Morokuma, G. A. Voth, P. Salvador, J. J. Dannenberg, V. G. Zakrzewski, S. Dapprich, A. D. Daniels, M. C. Strain, O. Farkas, D. K. Malick, A. D. Rabuck, K. Raghavachari, J. B. Foresman, J. V. Ortiz, Q. Cui, A. G. Baboul, S. Clifford, J. Cioslowski, B. B. Stefanov, G. Liu, A. Liashenko, P. Piskorz, I. Komaromi, R. L. Martin, D. J. Fox, T. Keith, M. A. Al-Laham, C. Y. Peng, A. Nanayakkara, M. Challacombe, P. M. W. Gill, B. Johnson, W. Chen, M. W. Wong, C. Gonzalez, and J. A. Pople, Gaussian, Inc., Wallingford CT, 2004.

13 Gaussian 09, Revision D.01, M. J. Frisch, G. W. Trucks, H. B. Schlegel, G. E. Scuseria, M. A. Robb, J. R. Cheeseman, G. Scalmani, V. Barone, B. Mennucci, G. A. Petersson, H. Nakatsuji, M. Caricato, X. Li, H. P. Hratchian, A. F. Izmaylov, J. Bloino, G. Zheng, J. L. Sonnenberg, M. Hada, M. Ehara, K. Toyota, R. Fukuda, J. Hasegawa, M. Ishida, T. Nakajima, Y. Honda, O. Kitao, H. Nakai, T. Vreven, J. A. Montgomery, Jr., J. E. Peralta, F. Ogliaro, M. Bearpark, J. J. Heyd, E. Brothers, K. N. Kudin, V. N. Staroverov, R. Kobayashi, J. Normand, K. Raghavachari, A. Rendell, J. C. Burant, S. S. Iyengar, J. Tomasi, M. Cossi, N. Rega, J. M. Millam, M. Klene, J. E. Knox, J. B. Cross, V. Bakken, C. Adamo, J. Jaramillo, R. Gomperts, R. E. Stratmann, O. Yazyev, A. J. Austin, R. Cammi, C. Pomelli, J. W. Ochterski, R. L. Martin, K. Morokuma, V. G. Zakrzewski, G. A. Voth, P. Salvador, J. J. Dannenberg, S. Dapprich, A. D. Daniels, Ö. Farkas, J. B. Foresman, J. V. Ortiz, J. Cioslowski, and D. J. Fox, Gaussian, Inc., Wallingford CT, 2009.

14 (*a*) C. P. Constantinides, P. A. Koutentis, H. Krassos, J. M. Rawson and A. J. Tasiopoulos, *J. Org. Chem.*, 2011, **76**, 2798; (*b*) C. P. Constantinides, P. A. Koutentis and J. M. Rawson, *Chem.-Eur. J.*, 2012, **18**, 7109; (*c*) C. P. Constantinides, P. A. Koutentis and J. M. Rawson, *Chem.-Eur. J.*, 2012, **18**, 15433; (*d*) C. P. Constantinides, E. Carter, D. M. Murphy, M. Manoli, G. M. Leitus, M. Bendikov, J. M. Rawson and P. A. Koutentis, *Chem. Commun.*, 2013, **49**, 8662.

15 (*a*) F. A. Neugebauer and I. Umminger, *Chem. Ber.*, 1980, **113**, 1205; (*b*) F. A. Neugebauer and G. Rimmler, *Magn. Reson. Chem.*, 1988, **26**, 595; (*c*) F. A. Neugebauer and I. Umminger, *Chem. Ber.*, 1981, **114**, 2423.

16 $A_N = Q_N.\rho_N$ where $A_N$ are the hfcc in Gauss; $Q_N = 21.2$ G (for N2 and N4) and $Q_N = 25$G (for N1).

17 H. M. McConnell, *J. Chem. Phys.*, 1958, **28**, 1188.

18 J. W. Hall, W. E. Marsh, R. R. Weller and W. E. Hatfield, *Inorg. Chem.*, 1981, **20**, 1033.
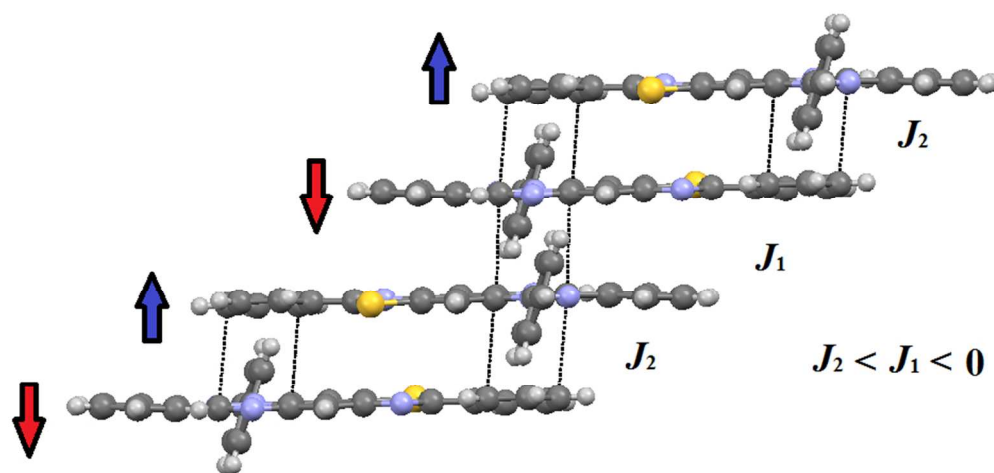
19 J. J. Novoa, M. Deumal and J. Jornet-Somoza, *Chem. Soc. Rev.*, 2011, **40**, 3182.

20 L. Noodleman, *J. Chem. Phys.*, 1981, **74**, 5737.

21 (*a*) X. Xu and W. A. Goddard III, *Proc. Natl. Acad. Sci. U.S.A.*, 2004, **101**, 2673; (*b*) Y. Zhao and D. G. Truhlar, *Theor. Chem. Acc.*, 2008, **120**, 215.

22 M. Deumal, J. J. Novoa, M. J. Bearpark, P. Celani, M. Olivucci and M. A. Robb, *J. Phys. Chem. A.*, 1988, **102**, 8404.

23 M. Mito, Y. Komorida, H. Tsuruda, J. S. Tse, S. Desgreniers, Y. Ohishi, A. A. Leitch, K. Cvrkalj, C. M. Robertson and R. T. Oakley, *J. Am. Chem. Soc.*, 2009, **131**, 16012.

249x116mm (96 x 96 DPI)